



OPEN ACCESS

EDITED BY

Chao Yang,
South China University of Technology,
China

REVIEWED BY

Pedro Brito,
Pontifícia Universidade Católica de
Minas Gerais, Brazil
Ubong Eduok,
Western University, Canada

*CORRESPONDENCE

Zhiwei Liu,
liuzhiwei@xjtu.edu.cn

SPECIALTY SECTION

This article was submitted to Mechanics
of Materials,
a section of the journal
Frontiers in Materials

RECEIVED 26 July 2022

ACCEPTED 01 September 2022

PUBLISHED 15 September 2022

CITATION

Zheng X, Yin H, Shu Y, Chu Z and Liu Z
(2022), The corrosion behavior and
tensile strength of the 2060 Al-Li alloy
with different heat treatments.
Front. Mater. 9:1003204.
doi: 10.3389/fmats.2022.1003204

COPYRIGHT

© 2022 Zheng, Yin, Shu, Chu and Liu.
This is an open-access article
distributed under the terms of the
[Creative Commons Attribution License
\(CC BY\)](https://creativecommons.org/licenses/by/4.0/). The use, distribution or
reproduction in other forums is
permitted, provided the original
author(s) and the copyright owner(s) are
credited and that the original
publication in this journal is cited, in
accordance with accepted academic
practice. No use, distribution or
reproduction is permitted which does
not comply with these terms.

The corrosion behavior and tensile strength of the 2060 Al-Li alloy with different heat treatments

Xingwei Zheng¹, Haohao Yin², Yan Shu³, Zhenhua Chu² and Zhiwei Liu^{4*}

¹College of Science, Donghua University, Shanghai, China, ²College of Engineering Science and Technology, Shanghai Ocean University, Shanghai, China, ³Ocean Science and Engineering College, Shanghai Maritime University, Shanghai, China, ⁴State Key Laboratory for Mechanical Behavior of Materials, School of Materials Science and Engineering, Xi'an Jiao Tong University, Xi'an, China

The structural safety and service life of civil aircraft can be decreased by corrosion damage to their aluminum components caused by long-term service in corrosive conditions. In this work, the effect of heat treatment on corrosion behavior and tensile strength was systematically analyzed for 2060 Al-Li alloy immersed in 3.5 wt% NaCl solution for different corrosion times. The results show that the corrosion depths of the 2060-T4 and 2060-T6 Al-Li alloys immersed for 720 h are 85 and 93 μm , respectively. The ultimate tensile strengths of 2060-T4 and 2060-T6 Al-Li alloys immersed for 720 h were reduced by 5.8 and 6.4%, respectively. Linear relationships between tensile strength and the corrosion depths of 2060-T4 and 2060-T6 Al-Li alloys were established as $\sigma_{res} = 486 - 0.33h$ and $\sigma_{res} = 547 - 0.35h$ respectively.

KEYWORDS

Al-Li alloy, corrosion, heat treatment, residual strength, corrosion depth

Introduction

As a light metallic material, aluminum-lithium (Al-Li) alloy is a primary candidate for a wide range of applications in the aeronautic industry owing to its lower density, better strength, and higher stiffness compared to the conventionally commercial 2XXX and 7XXX series aluminum alloys (Nayan et al., 2017; Zheng et al., 2018; Zheng et al., 2021). However, the addition of Li can increase the corrosion sensitivity of the resultant alloy due to its reactive nature, which is problematic when the Al-Li alloy is exposed to corrosive environments (Jiang et al., 2020). The corrosion behaviors of Al-Li alloys are currently being widely investigated. And the results show that the corrosion behaviors of Al-Li alloys are greatly influenced by their heat treatment (Jiang et al., 2020; Chen et al., 2021; Kuang et al., 2021), precipitates (Zhu et al., 2020; Xu et al., 2022), surface abrasion (Liu et al., 2018), and corrosion environment (Qin et al., 2021; Jiang et al., 2022; Guérin et al., 2015).

The structural components of civil aircraft made of aluminum alloys have a significant impact on their safety (Jiang et al., 2020; Zhu et al., 2020; Kuang et al., 2021; Yin et al., 2022). Corrosion is one of the main damage forms of aircraft aluminum structures and is

TABLE 1 The nominal and actual concentrations of chemical elements in 2060 alloy (in weight percent).

	Cu	Mn	Mg	Zn	Zr	Ag	Li	Al
Nominal	3.0–3.8	0.3–0.5	0.6–0.9	0.2–0.5	0.1–0.3	0.1–0.3	0.6–1.2	Bal
Actual	3.4	0.4	0.8	0.4	0.3	0.2	1.1	Bal

one of the main causes of aircraft faults and disasters. This is particularly the case in a long-term service in a coastal area enriched with plenty of salinity. The influence of corrosion on the mechanical properties, including tensile strength and fatigue performance, of aluminum structures is of considerable importance in the evaluation of the structural integrity of aircraft (Zhang et al., 2008). Holes, cracks and dents are the most common causes of tensile strength and fatigue life loss in the fuselage skin panels (Li et al., 2015a). The investigations on the corrosion of Al-Li alloys show that corrosion pits (holes on the surface) often form during the corrosion (Kuang et al., 2021; Zhu et al., 2020; Xu et al., 2022; Liu et al., 2018; Qin et al., 2021; Jiang et al., 2022; Guérin et al., 2015). Therefore, study on the relationship between corrosion pit and residual strength of Al-Li alloys is meaningful to extend their applications.

As a member of the third-generation Al-Li alloy, the 2060 alloy was invented by Alcoa in 2011. It was designed as a replacement, enabling prosperous applications in civil aircraft components conventionally made of commercial 2024 and 7,075 alloys (El-Aty et al., 2018). Which has been widely used to prepare the panels of civil aircraft at home and aboard and has been selected as the research object of this paper. The aim of this paper is to investigate the corrosion behavior and tensile strength of the third generation 2060 Al-Li alloys with different heat treatments, aiming to further promote their application in civil aircraft and marine engineering.

Experimental procedure and materials

The main alloying elements in the as-received 2060-T8 Al-Li alloy sheet (2 mm in thickness) are Cu, Mn and Mg, respectively. And its detailed composition tested by ICP-AES is shown in Table 1.

The 2060-T4 and 2060-T6 Al-Li alloys were prepared according to the previous work (Li et al., 2015b). At first, the as-received 2060-T8 Al-Li alloy was subjected to solution treatment (535 C, 30 min + water quenching) before aging treatment. Then the 2060-T6 Al-Li alloy was prepared by artificial aging treatment (165 C, 20 h). And the 2060-T4 Al-Li alloy was prepared by natural aging treatment (room temperature, 2 weeks) after solution treatment.

Square specimens with a side length of 10 mm were cut from the 2060-T6 and 2060-T4 Al-Li alloys. And then the specimens were cleaned by an ultrasonic cleaning machine. After that, all the

specimens with T4 or T6 heat treatment were ground and polished with 2000 # and 3000 # SiC sandpaper successively. Finally, the specimens were cleaned by an ultrasonic cleaning machine, and the specimens were dried with cold air before the immersion test. The electro-chemical behavior of the 2060 Al-Li alloy was tested by a Gamry Interface 600 plus potentiostat installed with a standard cell system consisting of three types of electrodes, i.e., the counter (platinum), the reference (silver chloride), and the working (2060 alloy), respectively. A region with an area of 1 cm² was exposed to a 3.5 wt% NaCl solution. Potentiodynamic polarization curves and electro-chemical impedance spectra were depicted for 2060-T4 and 2060-T6 alloys exposed for up to 720 h.

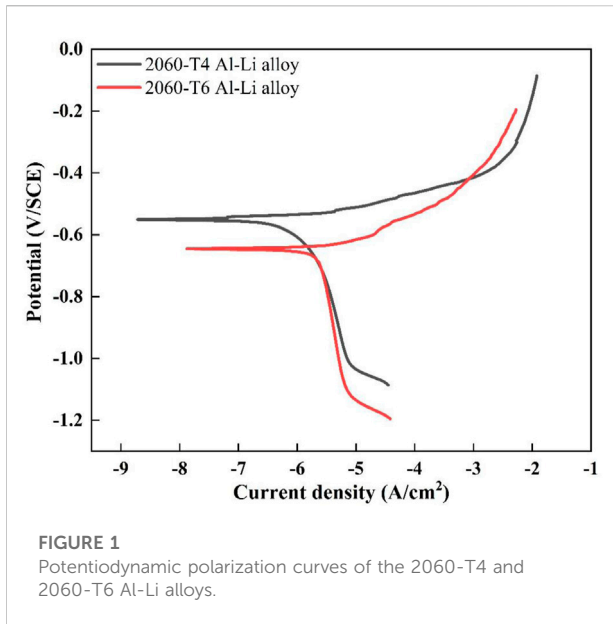
The tensile specimens were cut from the 2060 Al-Li alloy after T4 and T6 heat treatments along the rolling direction. The size of the tensile specimen was designed in accordance with ASTM E-8, and the detailed dimensions of the tensile specimen can be referred to in our previous work. The corrosion tests for the tensile specimens were repeated three times in the 3.5% NaCl solution refreshed every 7 days. The corrosion times for the corrosion test were designed to be 6, 24, 72, 168, 360, and 720 h, respectively. Subsequently, the tensile test was conducted on the Zwick/Roell Z050, and the strain rate was $5.556 \times 10^{-4} \text{ s}^{-1}$ in this work.

Corrosion products were removed from the surface of the sample according to the specification GB/T 16545-2015. In order to measure the corrosion depth of the corrosion pit, the same method as in Ref (Guérin et al., 2015; Liu et al., 2018). The corrosion depths of the samples immersed with different times were measured ten times, and the average value was recorded as the corrosion depth of the corresponding one. A scanning electron microscope (SEM, FEI Quanta-250) installed with an energy dispersive spectrum (EDS) apparatus was used to inspect the morphology of the corrosion on the corroded surface.

Results and discussion

Corrosion behavior of 2060-T4 and 2060-T6 Al-Li alloys

Corrosion potential is a parameter which can reflect the corrosion sensitivity of metallic materials under a liquid corrosive medium. In general, as the corrosion potential



increases, the corrosion sensitivity of the metallic material decreases. The polarization curves of 2060-T4 and 2060-T6 Al-Li alloys in a 3.5 wt% NaCl solution are shown in Figure 1. It can be seen that obvious passivation behavior can be observed in the polarization curves of the 2060-T4 and 2060-T6 Al-Li alloys. Electrochemical parameters obtained by Tafel fitting of the polarization curve of the 2060-T4 and 2060-T6 Al-Li alloys are shown in Table 2. The results show that the corrosion potential of 2060-T4 Al-Li alloy is slightly higher than that of the 2060-T6 Al-Li alloy. This means that the 2060-T4 Al-Li alloy has a slightly lower corrosion sensitivity than that of the 2060-T6 Al-Li alloy. And the corrosion current density of the 2060-T6 Al-Li alloy is higher than that of the 2060-T4 Al-Li alloy. The result is consistent with the result of corrosion potential. It is worth mentioning that the corrosion potentials of 2099-T4 and 2199-T6 Al-Li alloys are -0.648 V and -0.700 V, respectively (Meng, 2016). And the corrosion potentials of 2195-T4 and 2195-T6 Al-Li alloys are -0.885 V and -0.895 V, respectively (Gu, 2019). It can be seen that the corrosion potential of 2060 Al-Li alloy (as shown in table.2) is higher than that of the AA2099 Al-Li alloy. These results indicate that the corrosion resistance of the third generation 2060 Al-Li alloy is remarkably improved compared with the previous Al-Li alloy.

Electrochemical impedance spectroscopy (EIS) measurements were performed to evaluate the corrosion

resistance performance of the 2060 alloys in 3.5 wt% NaCl solution. Figure 2 shows the electrochemical impedance spectroscopy of 2060-T6 and 2060-T4 Al-Li alloys in 3.5 wt% NaCl solution. The results show that the impedance radius of the 2060-T6 Al-Li alloy is smaller than that of the 2060-T4 Al-Li alloy, which indicates that the corrosion resistance of the 2060-T4 Al-Li alloy is better than that of the 2060-T6 Al-Li alloy. Therefore, the results of electrochemical impedance spectroscopy are consistent with the results of potentiodynamic polarization curve. On the other hand, there are two capacitive reactance arcs in both of the 2060-T4 and 2060-T6 Al-Li alloys, which means that there are two-time constants during the corrosion of the 2060-T4 and 2060-T6 Al-Li alloys in 3.5 wt% NaCl solution. Thus, the equivalent circuit of the 2060-T4 and 2060-T6 Al-Li alloys immersed in 3.5 wt% NaCl solution is shown in Figure 3. Where R_s denotes the solution resistance. R_{ct} denotes the charge transfer resistance. CPE_f denotes a constant phase element between the solution and the passivation film. CPE_{ct} denotes a constant phase element between the solution and the electrode. And the electrochemical impedance spectroscopy parameters of 2060-T4 and 2060-T6 Al-Li alloys immersed in the 3.5% NaCl solution for different times are fitted based on the suggested equivalent circuit and listed in Table 3. It can be seen that the R_{ct} values of 2060-T4 and 2060-T6 Al-Li alloys are $34120 \Omega \text{ cm}^2$ and $13440 \Omega \text{ cm}^2$, indicating that the corrosion resistance of 2060-T4 Al-Li alloy is better than that of the 2060-T6 Al-Li alloy, which is consistent with the results of the electrochemical impedance spectroscopy.

Figure 4 shows the morphology of corrosion products on the surface of the 2060-T4 Al-Li alloy immersed in the 3.5 wt% NaCl solution for 0, 6, 24, 72, 168, and 720 h, respectively. No obvious corrosion products are observed as the immersion time was less than 24 h, and corrosion products begin to appear on the surface of the 2060-T4 Al-Li alloy. The surface of the 2060-T4 Al-Li alloy is completely covered by corrosion products as the immersion time is more than 72 h. The previous investigations on corrosion of Al-Li alloys in the NaCl solution showed that the corrosion product was mainly composed of Al, Cl, and O elements, and it has been identified that the corrosion product was $\text{Al}(\text{OH})_x\text{Cl}_{3-x}$ (Zheng et al., 2022). Figure 5 shows the corrosion morphology of the 2060-T4 Al-Li alloy after removing the corrosion products. It can be seen that some small corrosion pits are formed on the local surface of the 2060-T4 Al-Li alloy as the immersion time exceeds 6 h, and uniform corrosion pits are observed on the surface of the 2060-T4 Al-Li alloy as the

TABLE 2 Electrochemical parameters obtained by Tafel fitting of polarization curves of the 2060-T4 and 2060-T6 Al-Li alloys.

Temper	E_{corr}/V	$i_{\text{corr}}/\text{A}\cdot\text{cm}^{-2}$	BetaA/ $\text{mV}\cdot\text{dec}^{-1}$	BetaB/ $\text{mV}\cdot\text{dec}^{-1}$
T6	-0.645	3.09×10^{-6}	96.27	162.1
T4	-0.550	1.46×10^{-7}	80.65	114.5

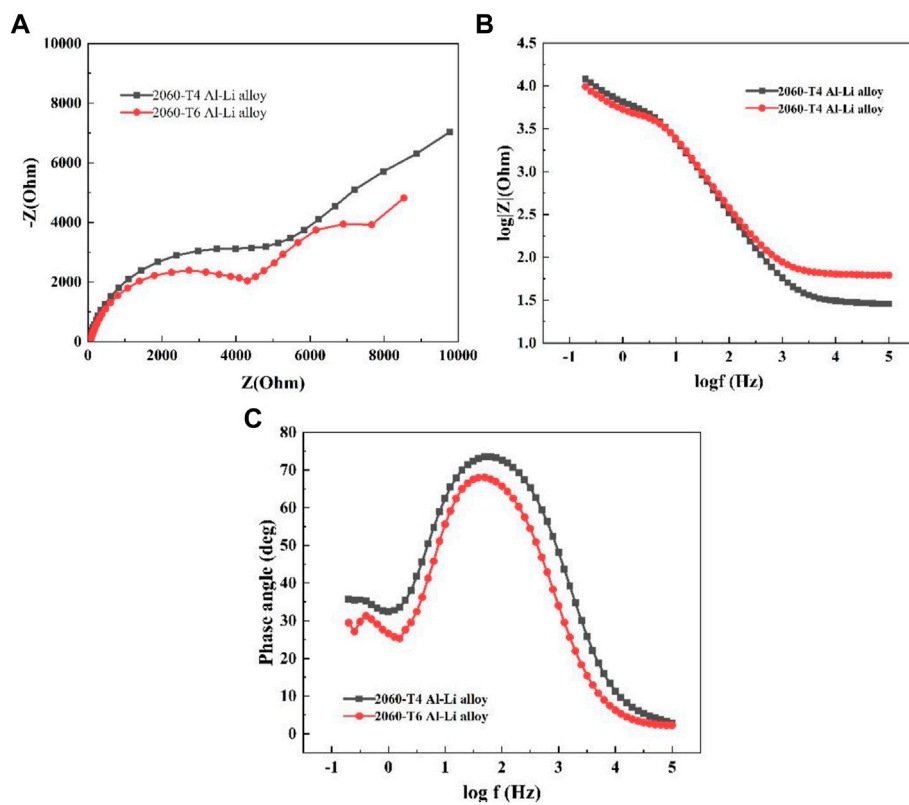


FIGURE 2
EIS plots of two 2060 Al-Li alloys, (A) Nyquist plots, (B) Bode impedance magnitude plots, (C) Bode phase angle plots.

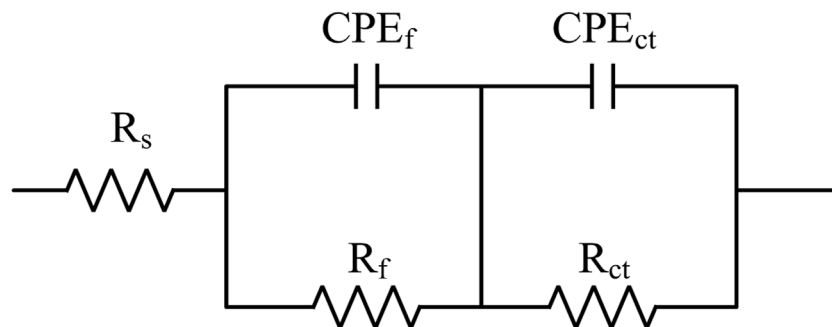


FIGURE 3
The equivalent electrical circuit.

immersion time exceeds 168 h. The size of corrosion pits of the 2060-T4 Al-Li alloy increases with an increase of immersion time.

Figure 6 shows the morphology of corrosion products on the surface of the 2060-T6 Al-Li alloy after being immersed in the 3.5 wt % NaCl solution for 0, 6, 24, 72, 168, and 720 h, respectively. It can

be seen that corrosion products of 2060-T6 Al-Li alloy begin to appear as the immersion time exceeds 6 h, which is much shorter than that of 2060-T4 Al-Li alloy (24 h). This result indicates that the corrosion resistance of the 2060-T4 Al-Li alloy is better than that of the 2060-T6 Al-Li alloy. The surface of the 2060-T6 Al-Li alloy is completely covered by corrosion products as the immersion time

TABLE 3 Equivalent electrical circuit parameter fitting value of three heat-treated state 2060 Al-Li alloy samples in 3.5 wt% NaCl solution.

Temper	$R_s/\Omega\cdot\text{cm}^2$	$R_{ct}/\Omega\cdot\text{cm}^2$	$R_f/\Omega\cdot\text{cm}^2$
T6	62.60	13440	4449
T4	28.41	34120	4304

exceeds 72 h. Figure 7 shows the corrosion morphology of the surface of the 2060-T6 Al-Li alloy after removing the corrosion products. It can be seen that the distribution of corrosion pits on the surface of the 2060-T6 Al-Li alloy is relatively concentrated, while the distribution of corrosion pits on the surface of 2060-T4 Al-Li alloy is relatively uniform (as shown in Figure 4).

Tensile strength of 2060-T4 and T6 Al-Li alloys

The residual tensile strength of light-weight Al-Li alloy subjected to corrosion is the key to damage tolerance of the alloy designed for aircraft applications (Alexopoulos et al., 2016; Charalampidou et al., 2021). And it is close related to the heat treatment. Consequently, it is worthwhile to investigate the effect of corrosion on the tensile strength of 2060 Al-Li

alloy with different heat treatments. The relationship of the 2060-T4 Al-Li alloy between the tensile strength and immersion time is shown in Figure 8. It can be seen that the strength of the 2060-T4 Al-Li alloy, including yield strength and ultimate tensile strength, decreases with an increase of immersion time, and it can be divided into two different stages. First, the mechanical properties of the 2060-T4 Al-Li alloy decrease rapidly as the immersion time is less than 360 h. Second, the mechanical properties of the 2060-T4 Al-Li alloy decrease gently as the immersion time exceeds 360 h. In detail, the ultimate tensile strength decreases from 485 to 457 MPa, and the corresponding decrease rate is 5.8%. The change trends of tensile strength and yield strength of 2060-T4 Al-Li alloy with immersion time is fitted according to Figure 8. The corresponding relationships can be expressed as (Eqs. 1, 2), respectively.

$$\sigma_b = 27.68 \times \exp^{(-t/147.20)} + 455.31 \quad (1)$$

$$\sigma_s = 7.93 \times \exp^{(-t/197.84)} + 301.63 \quad (2)$$

The change trends of tensile strength and yield strength of 2060-T6 Al-Li alloy with immersion time is fitted according to Figure 9. It can be seen that the change trend of the 2060-T6 Al-Li alloy is almost the same as that of the 2060-T4 Al-Li alloy. However, the rates of decrease in ultimate tensile strength and yield strength are 6.4 and 10.8%, respectively. Which are slightly higher than that of the 2060-T4 Al-Li alloy. The relationships

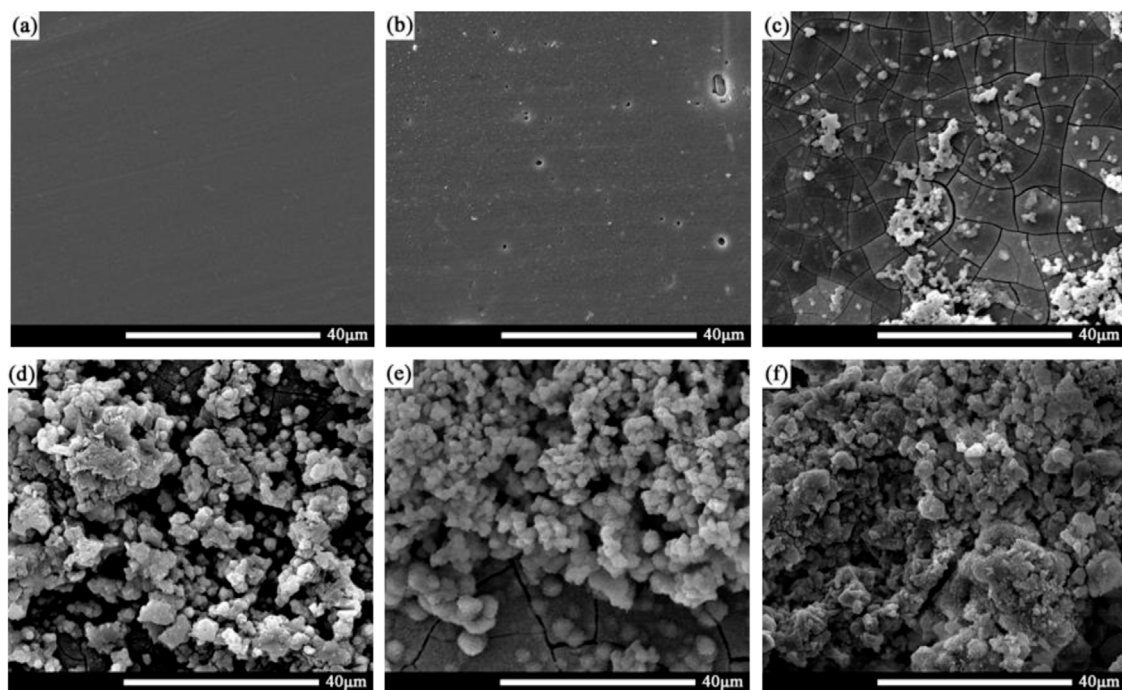


FIGURE 4 Corrosion products of 2060-T4 Al-Li alloy samples with different immersion time, (A) 0 h, (B) 6 h, (C) 24 h, (D) 72 h, (E) 168 h, (F) 720 h.

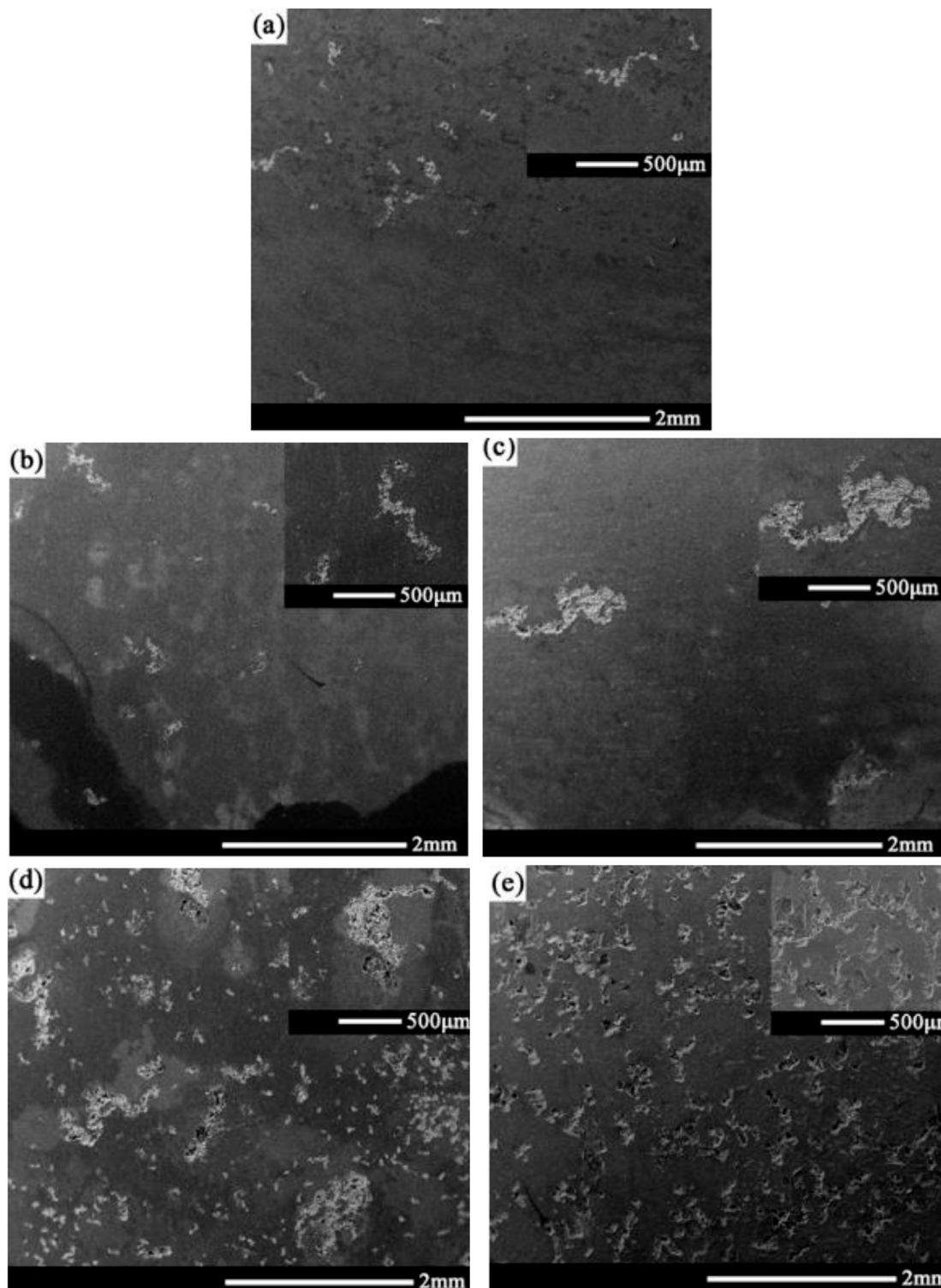


FIGURE 5
Corrosion morphology of 2060-T4 Al-Li alloy with different immersion time after removing corrosion products, (A) 6 h, (B) 24 h, (C) 72 h, (D) 168 h, (E) 720 h.

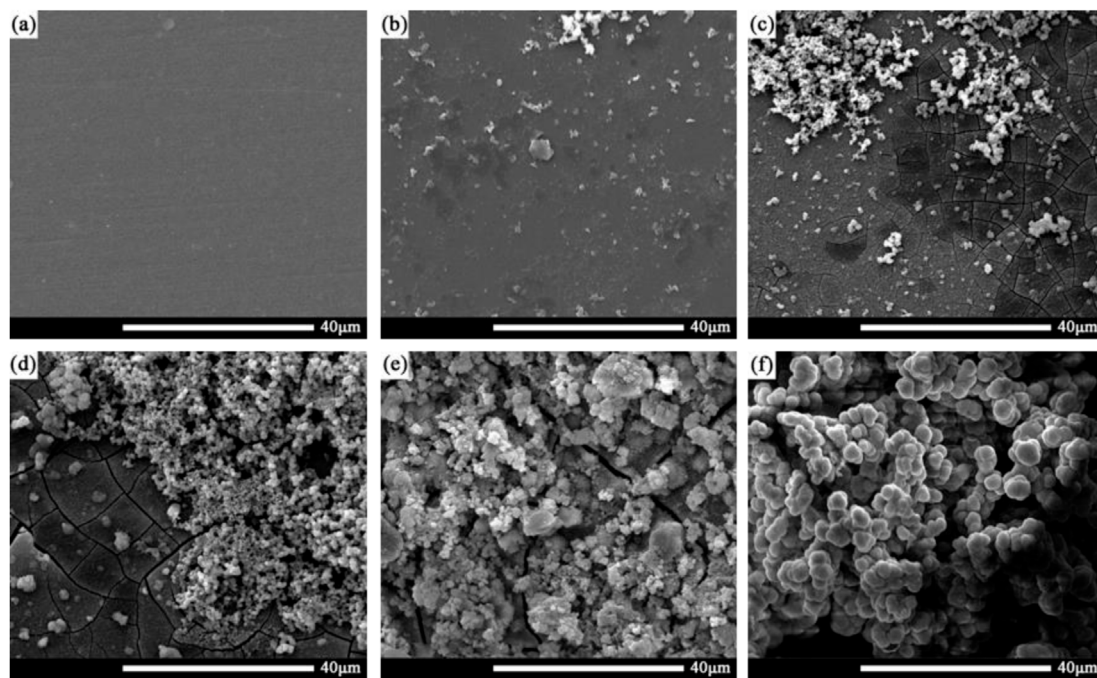


FIGURE 6
Corrosion product of 2060-T6 Al-Li alloy samples with different immersion time, (A) 0 h, (B) 6 h, (C) 24 h, (D) 72 h, (E) 168 h, (F) 720 h.

between ultimate tensile strength (yield strength) and immersion time can be expressed as Eqs. 3, 4, respectively.

$$\sigma_b = 37.60 \times \exp^{-t/405.98} + 502.65 \quad (3)$$

$$\sigma_s = 7.93 \times \exp^{-t/197.84} + 301.63 \quad (4)$$

Correlation between tensile strength and pit size

The size of the corrosion pit is an important index to characterize the severity of corrosion. Figure 10 shows the corrosion depth of the 2060-T4 Al-Li alloy after immersion in 3.5 wt% NaCl solution for 0, 6, 24, 72, 168, 360, and 720 h, respectively. The results show that the corrosion depth of the 2060-T4 Al-Li alloy increases rapidly as the immersion time is less than 360 h. While the corrosion depth of the 2060-T4 Al-Li alloy remains nearly stable as the immersion time exceeds 360 h. The maximum corrosion depth of the 2060-T4 Al-Li alloy is about 85 μm as the immersion time is 720 h. The result is consistent with the variation trend of tensile strength. It indicates that the tensile strength of the 2060-T4 Al-Li alloy is closely related to the corrosion depth. The correlation between the corrosion depth and the tensile strength of the 2060-T4 Al-Li alloy is shown in Figure 10. It can be seen that the tensile strength

of the 2060-T4 Al-Li alloy decreases linearly with an increase of corrosion depth. The relationships between tensile strength (ultimate tensile strength) and corrosion depth can be expressed as Eq. 5.

$$\sigma_{res} = 486 - 0.33h \quad (5)$$

where, σ_{res} is tensile strength, h is the corrosion depth of 2060-T4 Al-Li alloy.

Figure 11 shows the corrosion depth of the 2060-T6 Al-Li alloy after immersion in 3.5 wt% NaCl solution for 0, 6, 24, 72, 168, 360 and 720 h, respectively. No obvious difference is observed in the variation trend of corrosion depth with immersion time between the 2060-T6 Al-Li alloy and the 2060-T4 Al-Li alloy. However, the maximum corrosion depth of the 2060-T6 Al-Li alloy is about 93 μm as the immersion time is 720 h, which is slightly higher than that of the 2060-T4 Al-Li alloy. The correlation between the corrosion depth and the tensile strength of the 2060-T6 Al-Li alloy is shown in Figure 11. It can be seen that the tensile strength of the 2060-T6 Al-Li alloy also decreases linearly with an increase of the corrosion depth. The relationships between tensile strength (ultimate tensile strength) of the 2060-T6 Al-Li alloy and the corrosion depth can be expressed as Eq. 6.

$$\sigma_{res} = 547 - 0.35h \quad (6)$$

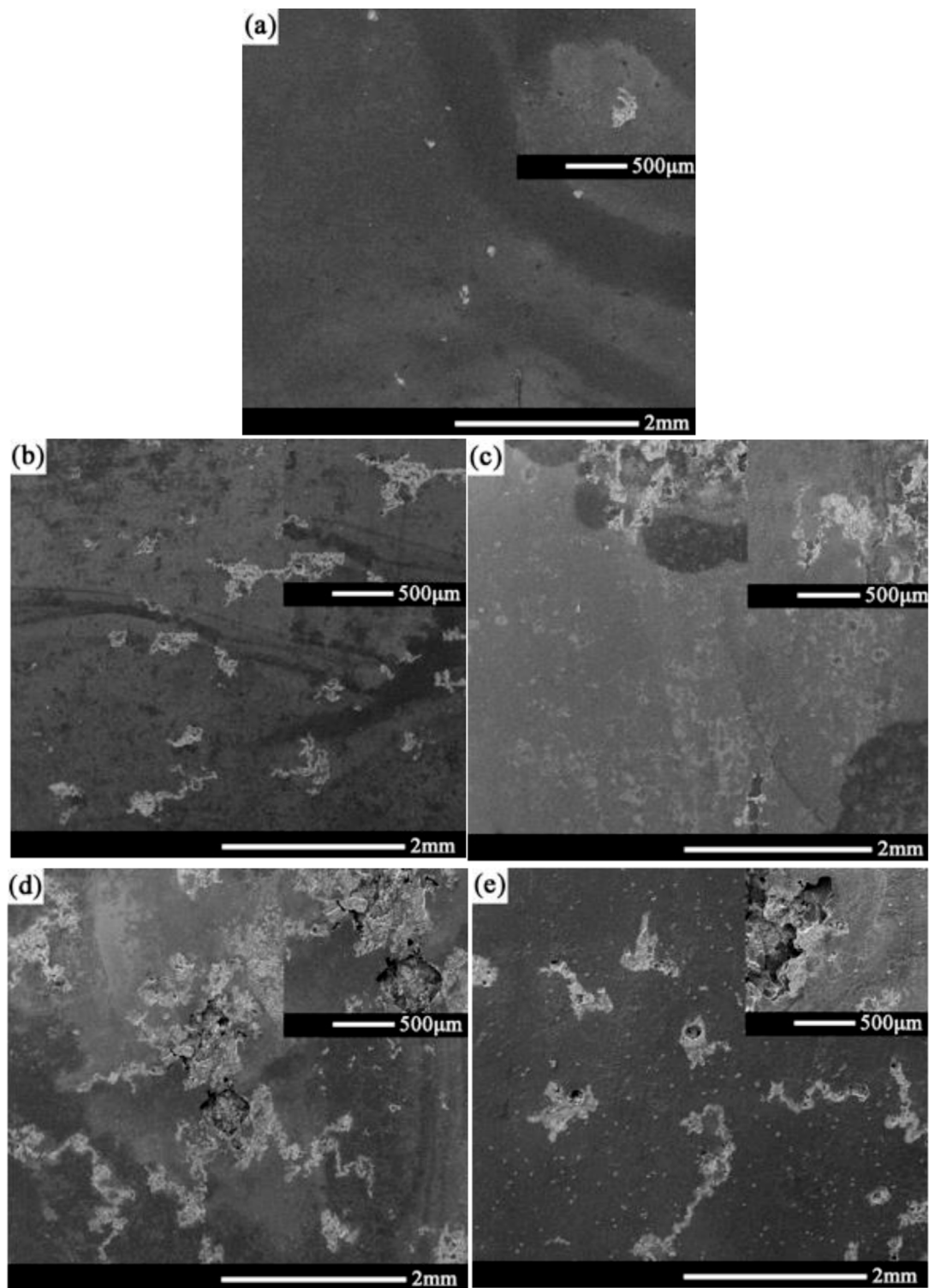


FIGURE 7
Corrosion morphology of 2060-T6 Al-Li alloy with different immersion time after removing corrosion products, (A) 6 h, (B) 24 h, (C) 72 h, (D) 168 h, (E) 720 h.

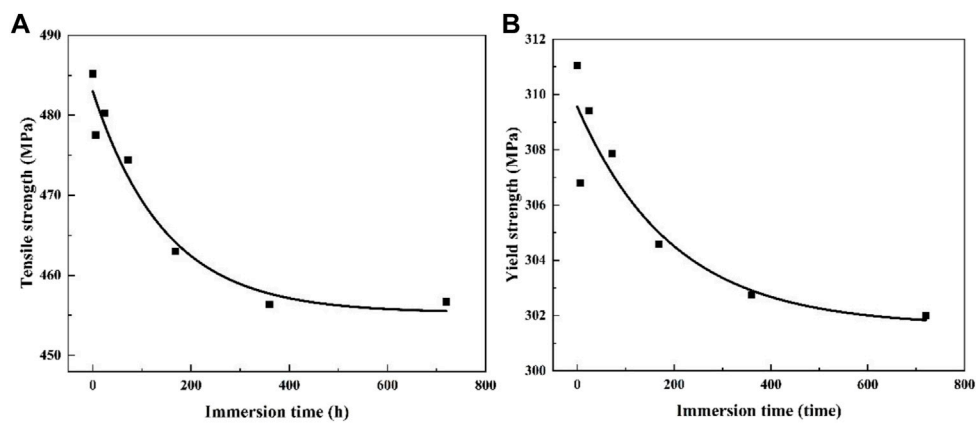


FIGURE 8
The trend of mechanical properties of 2060-T4 Al-Li alloy with immersion time and its fitting curve, (A) tensile strength, (B) yield strength.

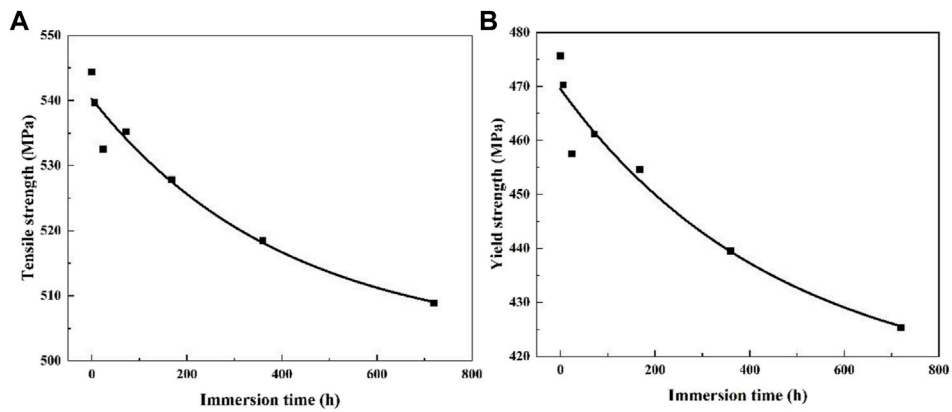


FIGURE 9
The trend of mechanical properties of 2060-T6 Al-Li alloy with immersion time and its fitting curve, (A) tensile strength, (B) yield strength.

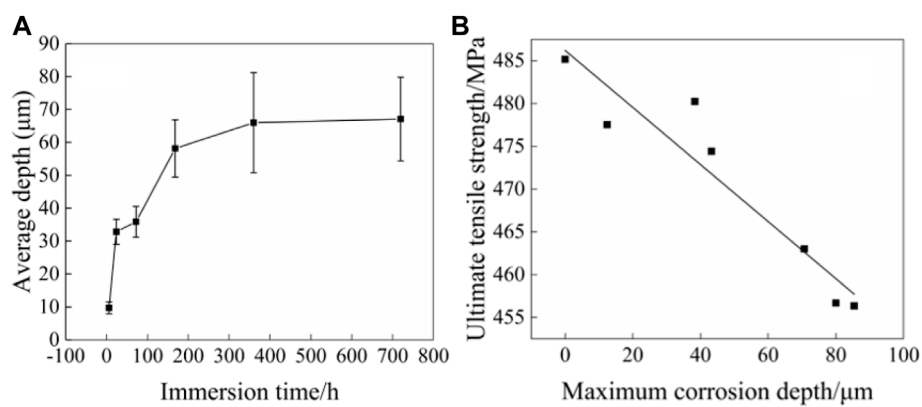


FIGURE 10
Correlation between corrosion depth and tensile strength of 2060-T4 Al-Li alloy immersed for 6, 24, 72, 168, 360 and 720 h in 3.5wt% NaCl solution. (A) Corrosion depth vs immersion time, (B) ultimate tensile strength vs corrosion depth.

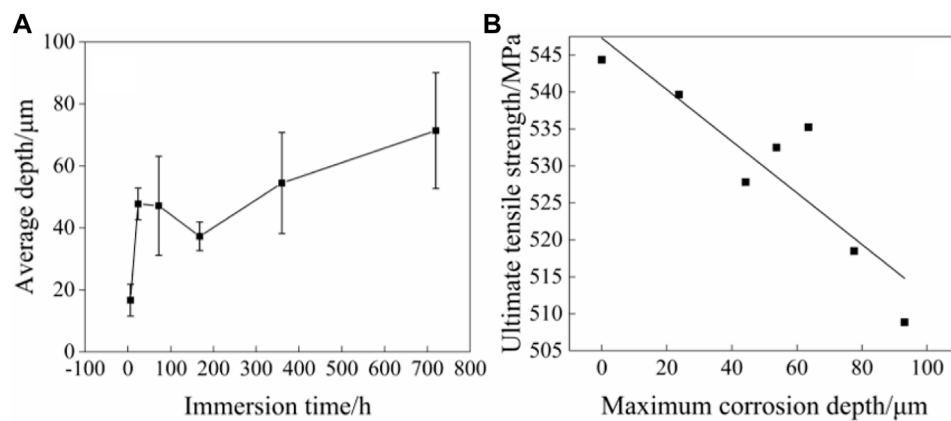


FIGURE 11

Correlation between corrosion depth and tensile strength of 2060-T6 Al-Li alloy immersed for 6, 24, 72, 168, 360 and 720 h in 3.5wt% NaCl solution. (A) Corrosion depth vs immersion time, (B) ultimate tensile strength vs corrosion depth.

Conclusion

The effect of heat treatment on the corrosion behavior and tensile strength was studied for 2060-T4 and 2060-T6 Al-Li alloys immersed in 3.5 wt% NaCl solution for different corrosion times. The main conclusions can be drawn as follows.

- 1) The ultimate tensile strengths of the 2060-T4 and 2060-T6 Al-Li alloys were reduced by 5.8 and 6.4% as the immersion time is 720 h.
- 2) The eletro-chemical behaviors of 2060-T4 and 2060-T6 Al-Li alloys indicate the corrosion products were formed gradually, which can prevent the 2060 Al-Li alloy from corrosion. And the corrosion resistance of 2060-T4 Al-Li alloy is better than that of 2060-T6 Al-Li alloy.
- 3) Linear relationships between tensile strength and the corrosion depths of 2060-T4 and 2060-T6 Al-Li alloys were established as $\sigma = 547 - 0.35h$ and $\sigma = 486 - 0.33h$, respectively.

Data availability statement

The original contributions presented in the study are included in the article/Supplementary Material, further inquiries can be directed to the corresponding author.

Author contributions

XZ: Methodology, Conceptualization, Writing-original draft. HY: Analysis, Writing-reviewing andamp; editing. YS: Analysis,

editing. ZC: Analysis, editing ZL: Conceptualization, Data curation, Visualization, Analysis.

Funding

This project was supported by the Fundamental Research Funds for the Central Universities (2232021D-27), State Key Laboratory for Mechanical Behavior of Materials (20222418) and Foundation Strengthening Program in the Technical Field Funds (2020-JCJQ-JJ-316).

Conflict of interest

The authors declare that the research was conducted in the absence of any commercial or financial relationships that could be construed as a potential conflict of interest.

Publisher's note

All claims expressed in this article are solely those of the authors and do not necessarily represent those of their affiliated organizations, or those of the publisher, the editors and the reviewers. Any product that may be evaluated in this article, or claim that may be made by its manufacturer, is not guaranteed or endorsed by the publisher.

References

- Alexopoulos, N. D., Proiou, A., Dietzel, W., Blawert, C., Heitmann, V., Zheludkevich, M., et al. (2016). Mechanical properties degradation of (Al-Cu-Li) 2198 alloy due to corrosion exposure. *Procedia Struct. Integr.* 2, 597–603. doi:10.1016/j.prostr.2016.06.077
- Charalampidou, C., Dietzel, W., Zheludkevich, M., Kourkoulis, S. K., and Alexopoulos, N. D. (2021). Corrosion-induced mechanical properties degradation of Al-Cu-Li (2198-T351) aluminium alloy and the role of side-surface cracks. *Corros. Sci.* 183, 109330. doi:10.1016/j.corsci.2021.109330
- Chen, X., Ma, X., Zhao, G., Wang, Y., and Xu, X. (2021). Effects of re-solution and re-aging treatment on mechanical property, corrosion resistance and electrochemical behavior of 2196 Al-Cu-Li alloy. *Mat. Des.* 204, 109662. doi:10.1016/j.matdes.2021.109662
- El-Aty, A. A., Xu, Y., Guo, X., Zhang, S., Ma, Y., and Chen, D. (2018). Strengthening mechanisms, deformation behavior, and anisotropic mechanical properties of Al-Li alloys: A review. *J. Adv. Res.* 10, 49–67. doi:10.1016/j.jare.2017.12.004
- Gu, X. (2019). *The effect of heat treatment on microstructure and properties of spray forming 2195 Al-Li alloy*. Zhenjiang, Jiangsu: Jiang Su University.
- Guérin, M., Alexis, J., Andrieu, E., Blanc, C., and Odemer, G. (2015). Corrosion-fatigue lifetime of Aluminium-Copper-Lithium alloy 2050 in chloride solution. *Mat. Des.* 87, 681–692. doi:10.1016/j.matdes.2015.08.003
- Jiang, Y., Xi, J., Du, L., Lei, W., Xing, J., Liu, C., et al. Time-varying electrochemically heterogeneous entities during the microgalvanic corrosion associated with nanoscale precipitates in an Al-Cu-Li alloy. *Corros. Sci.* (2022) 206, 110542. doi:10.1016/j.corsci.2022.110542
- Jiang, B., Wang, H., Tian, Y., Yi, D., Liu, H., and Hu, Z. (2020). Effects of aging time on corrosion behavior of an Al-Cu-Li alloy. *Corros. Sci.* 173, 108759. doi:10.1016/j.corsci.2020.108759
- Kuang, Q., Wang, R., Peng, C., Cai, Z., Feng, Y., and Wang, X. (2021). Influence of aging treatment on the microstructure, mechanical properties and corrosion behavior of spray deposited Al-Mg-Li-Sc-Zr alloy. *J. Alloys Compd.* 881, 160664. doi:10.1016/j.jallcom.2021.160664
- Li, H.-G., Ling, J., Xu, Y.-W., Sun, Z.-G., Liu, H.-B., Zheng, X.-W., et al. (2015). Effect of aging treatment on precipitation behavior and mechanical properties of a novel aluminum–lithium alloy. *Acta Metall. Sin.* 28, 671–677. doi:10.1007/s40195-015-0244-6
- Li, Z., Zhang, D., Peng, C., Ma, C., Zhang, J., Hu, Z., et al. (2015). The effect of local dents on the residual ultimate strength of 2024-T3 aluminum alloy plate used in aircraft under axial tension tests. *Eng. Fail. Anal.* 48, 21–29. doi:10.1016/j.engfailanal.2014.08.006
- Liu, J., Zhao, K., Yu, M., and Li, S. (2018). Effect of surface abrasion on pitting corrosion of Al-Li alloy. *Corros. Sci.* 138, 75–84. doi:10.1016/j.corsci.2018.04.010
- Meng, X. *Study on the effect of heat treatment and pre-deformation on localized corrosion behavior of AA2099 Al-Li alloy*. Chongqing, China: Chongqing University of Technology. 2016.
- Nayan, N., Murty, S. V. S. N., Chhangani, S., Prakash, A., Prasad, M. J. N. V., and Samajdar, I. (2017). Effect of temperature and strain rate on hot deformation behavior and microstructure of Al-Cu-Li alloy. *J. Alloys Compd.* 723, 548–558. doi:10.1016/j.jallcom.2017.06.165
- Qin, Y., Wu, G., Atrens, A., Zhang, X., Zhang, L., and Ding, W. (2021). Effect of NaOH concentration on microstructure and corrosion resistance of MAO coating on cast Al-Li alloy. *Trans. Nonferrous Metals Soc. China* 31, 913–924. doi:10.1016/s1003-6326(21)65549-8
- Xu, X., Hao, M., Chen, J., He, W., Li, G., Li, K., et al. (2022). Role of constituent intermetallic phases and precipitates in initiation and propagation of intergranular corrosion of an Al-Li-Cu-Mg alloy. *Corros. Sci.* 201, 110294. doi:10.1016/j.corsci.2022.110294
- Yin, H. Study on corrosion behavior and residual strength of a New Al-Li alloy Shanghai: Shanghai ocean university 2021.
- Zhang, Y., Lv, G., Wang, H., Si, B., and Cheng, Y. (2008). Corrosion damage evolution and residual strength of corroded aluminum alloys. *J. Univ. Sci. Technol. Beijing Mineral Metallurgy Material* 15, 430–433. doi:10.1016/s1005-8850(08)60081-x
- Zheng, X. W., Luo, P., Chu, Z. H., Xu, J. X., and Wang, F. H. (2018). Plastic flow behavior and microstructure characteristics of light-weight 2060 Al-Li alloy. *Mater. Sci. Eng. A* 736, 465–471. doi:10.1016/j.msea.2018.09.010
- Zheng, X. W., Luo, P., Yue, G. Q., and Hu, Y. X. (2021). Analysis of microstructure and high-temperature tensile properties of 2060 Al-Li alloy strengthened by laser shock peening. *J. Alloys Compd.* 860, 158539. doi:10.1016/j.jallcom.2020.158539
- Zhu, Y., Poplawsky, J. D., Li, S., Unocic, R. R., Bland, L. G., Taylor, C. D., et al. (2020). Localized corrosion at nm-scale hardening precipitates in Al-Cu-Li alloys. *Acta Mat.* 189, 204–213. doi:10.1016/j.actamat.2020.03.006